RSC Advances

ROYAL SOCIETY OF CHEMISTRY

www.rsc.org/advances

Graphical Abstract

A new rhodamine-derived fluorescent chemodosimeter for Cu^{2+} in aqueous solution and its application in living cell imaging

Ying-Ying Zhu, Xuan Zhang*, Hua Guo, Zhi-Jia Zhu

College of Chemistry, Chemical Engineering & Biotechnology, and National Engineering Research Center for Dyeing and Finishing of Textiles, Donghua University, Shanghai 201620, China.

*Corresponding author. Tel.: +86 21 67792619; *E-mail address:* xzhang@dhu.edu.cn

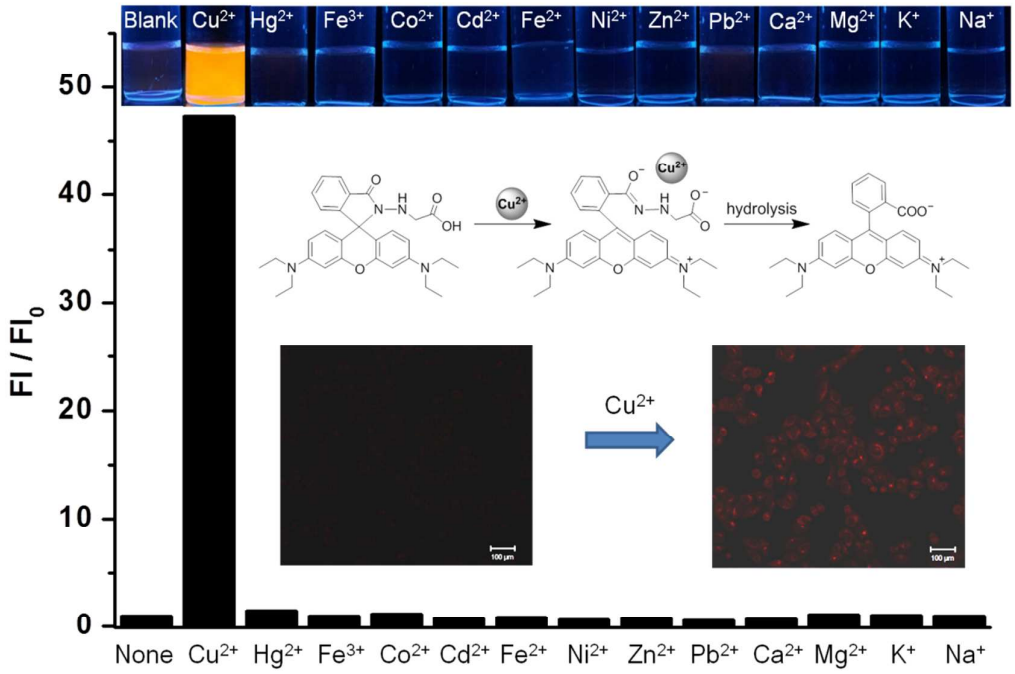

A new rhodamine-derived fluorescent chemodosimeter for Cu^{2+} in aqueous solution and its application in living cell imaging

Ying-Ying Zhu, Xuan Zhang*, Hua Guo, Zhi-Jia Zhu

College of Chemistry, Chemical Engineering & Biotechnology, and National Engineering Research Center for Dyeing and Finishing of Textiles, Donghua University, Shanghai 201620, China.

Tel.: +86 21 67792619; *E-mail address:* xzhang@dhu.edu.cn

Abstract

A new rhodamine-derived fluorescent chemodosimeter (**1**) for Cu^{2+} was synthesized, where a carboxylic acid group was introduced into rhodamine B hydrazide to enhance its water solubility. The probe **1** was weakly fluorescent but displayed a Cu^{2+}-selective fluorescence enhancement in aqueous solution. It was found that a 1:1 complex was formed between the probe **1** and Cu^{2+} in CH_3CN and rapidly converted into the parent rhodamine molecule upon addition of water. Thus a sensing mechanism of coordination-promoted hydrolysis was proposed based on ESI-MS analysis and DFT calculation. The present probe works in a near pure water solution (only containing 1% CH_3CN as co-solvent), with visible excitation/emission wavelength and a wide pH range of 6–10, making it suitable for fluorescence imaging of Cu^{2+} in the living cells.

1. Introduction

It has been known that copper is not only essential in living systems, but also toxic and hence capable of causing serious diseases.[1,2] Therefore the development of various selective and sensitive

methods for copper ion (Cu^{2+}) detection in solution and bio-systems has attracted much attention.[3–6] Especially, the fluorometric assays become more popular due to the fluorescence technique is simple, sensitive, selective, and easy to realize visualization by fluorescence imaging.[3–9] Cu^{2+} generally acts as a fluorescence quencher due to its paramagnetic nature that leads to an undesired low fluorescence signal outputs (turn-off).[4,5] Recent research interests are therefore mainly focused on the design of turn-on type small molecular fluorescent probe for Cu^{2+} with benefits for a bright fluorescence imaging.[4–9] For the sake of practical applications in biospecimens, good water-solubility, physiological working pH condition, and visible excitation and emission wavelengths are basically preferred performances for fluorescent probes.[8]

Fluorescent rhodamine dyes have excellent photophysical performances, such as visible excitation and emission wavelengths, high fluorescence quantum yield, and have been extensively used as biomolecular labels.[10,11] Recently, rhodamine-derived turn-on fluorescent probes have gathered considerable attention for metal cations such as Cu^{2+}, Hg^{2+}, Fe^{3+} and others,[12–30] based on the change in structure between spirocyclic and open-cycle forms. The free rhodamine-derived fluorescent probes usually are weakly fluorescent, but show a strong fluorescence enhancement upon addition of metal cation via reversible binding interaction (so-called chemosensor) or irreversible chemical reaction (so-called chemodosimeter).[4,8,9,12–14] However, many rhodamine-based fluorescent probes for Cu^{2+} usually worked in a pure organic solvent or an aqueous solution containing large amounts of organic components,[15–23, 31–40] which is undesired for a potential application in biological samples. Because of their high sensitivity and specific selectivity, the design and synthesis of chemodosimeters for fluorescence bioimaging have attracted increasing attention and become a very active field.[4,8,41,42] To date, a few rhodamine-based chemodosimeters for Cu^{2+} have reported, but

these probes were operated in 100% CH_3CN,[40] or aqueous solutions containing 80%,[35] 50%,[33, 37–39] 30%,[32] 20%, [31,36] and 10%[34] organic components, respectively.

Here we designed and facilely synthesized a novel rhodamine-based chemodosimeter **1** (Scheme 1), where a carboxylic acid group was introduced into rhodamine B hydrazide to enhance its water solubility. The probe **1** showed a highly selective fluorescent response toward Cu^{2+} in a near pure aqueous solution (only containing 1% CH_3CN as co-solvent) with a broad pH range of 6–10. Based on its promising performance, the probe **1** was further used for fluorescence imaging of Cu^{2+} in living cells.

2. Experimental

2.1. Materials and methods

Rhodamine B, hydrazine hydrate, *t*-butyl bromoacetate, and all organic solvents (AR) were purchased from Sinopharm Chemical Reagents Co. (Shanghai, China) and used as received. The solutions of metal cations were prepared by dissolving the corresponding perchlorate (Cu^{2+}, Hg^{2+}, Mg^{2+}, K^{+}, and Na^{+}), chloride (Co^{2+}, Ni^{2+}, Fe^{2+}, Zn^{2+}, Ca^{2+}) or nitrate (Fe^{3+}, Cd^{2+}, Pb^{2+}) salts with deionized water. The stock solution of probe **1** (1 mM) was prepared in CH_3CN and the working solution was obtained by dilution with Tris-HCl buffer solution (pH = 7.4, 10 mM).

Absorption and fluorescence spectra were recorded on a Persee TU-1901 and Hitachi F-7000 (Ex / Em slit widths: 2.5 nm) spectrophotometers with a 1 cm path length quartz cell, respectively. ESI-MS and MALDI-TOF-MS spectra were obtained on a Varian 310 and AB Sciex 4700 MALDI TOF/TOF^{TM} mass spectrometers, respectively. ^{1}H NMR and ^{13}C NMR spectra were measured on a Bruker AVANCE III 400 MHz spectrometer with TMS as standard. The pH was adjusted by using

Mettler Toledo pH Meter. Fluorescence imaging experiments for living cells were carried out with a Carl Zeiss LSM 700 laser scanning confocal microscope.

The DFT calculation for ground state structures of probe **1** and its Cu^{2+} complex were performed with Gaussian 09 program package,[43] at B3LYP level with the basis sets of 6-31G(d) for the C and H atoms, 6-31+G(d) for the O and N atoms, and LANL2DZ for Cu^{2+}, respectively.

2.2. Synthetic procedures

The total synthetic procedures are shown in Scheme 1.

(Scheme 1.)

Rhodamine B hydrazide **3** was synthesized by following the reported procedure.[16]

*Synthesis of **2***: Rhodahmine B hydrazide **3** (0.97 g, 2 mmol) was dissolved in CH_3CN (30.0 mL) and then K_2CO_3 (0.55 g, 4 mmol) and *t*-butyl bromoacetate (1.2 ml, 8 mmol) were added. The mixture solution was refluxed for 36 h under dry N_2 atmosphere and cooled to room temperature. The solid was removed by filtration and the filtrate was concentrated by rotary evaporation under reduced pressure. The obtained residue was subjected to column chromatography (silica gel, ethyl acetate / hexane = 2 / 1, v / v) to get pure compound **2** as a white solid (0.42 g, 37 %).^{1}H NMR (400 MHz, $CDCl_3$), δ (ppm): 1.16 (t, J = 4.0 Hz, 12 H), 1.38 (s, 9 H), 3.33 (m, 10 H), 4.70 (t, J = 4.0 Hz, 1 H), 6.28 (d, J = 8.0 Hz, 2 H), 6.40 (s, 2 H), 6.46 (d, J = 8.0 Hz, 2 H), 7.08 (d, J = 8.0 Hz, 1 H), 7.44 (t, J = 4.0 Hz, 2 H), 7.90 (d, J = 8.0 Hz, 1 H). ^{13}C NMR (100 MHz, $CDCl_3$), δ (ppm): 12.63, 28.05, 44.35, 52.65, 65.42, 81.34, 98.03, 105.55, 107.87, 122.80, 123.92, 128.03, 128.39, 129.92, 132.67, 148.71, 151.91, 153.64, 166.44, 169.3. MALDI-TOF mass $(M + H)^+$: *m/z* calcd for $C_{34}H_{43}N_4O_4$:

571.32; found 571.41.

*Synthesis of **1***: The compound **2** (0.28 g, 0.5 mmol) was dissolved in CH_2Cl_2 (2.0 mL) and trifluoroacetic acid (2.0 mL) and stirred at room temperature (300 K) for 24 h. The solvent was then removed under reduced pressure and the residue was washed with diethylether and dried in vacuo, affording **1** as a purple powder (0.23 g, 90%). ^{1}H NMR (400 MHz, $CDCl_3$), δ (ppm): 1.2 (t, J = 8.0 Hz, 12 H), 3.28 (s, 2 H), 3.27 (t, J = 8.0 Hz, 8 H), 6.33 (d, J = 8.0 Hz, 2 H), 6.42 (d, J = 8.0 Hz, 4 H), 7.16 (d, J = 8.0 Hz, 1 H), 7.56 (m, 2 H), 8.00 (d, J = 8.0 Hz, 1 H). ^{13}C NMR (400 MHz, $CDCl_3$), δ (ppm): 12.54, 44.53, 52.53, 66.77, 97.96, 103.21, 108.56, 123.60, 124.13, 128.33, 128.64, 128.75, 133.81, 149.17, 151.29, 153.86, 168.61, 172.15. ESI-MS $(M + H)^+$: *m/z* calcd for $C_{30}H_{35}N_4O_4$: 515.3; found 515.2.

3. Results and discussion

3.1. Selective fluorescence responses toward Cu^{2+}

Fig. 1 showed the fluorescence spectra of **1** (10 μM) in the presence of 20 equiv various metal cations in Tris-HCl buffer solutions (pH = 7.4, containing 1% CH_3CN as co-solvent). The probe **1** only is almost non-fluorescent, but around 50-fold fluorescent enhancement at 576 nm is selectively observed upon addition of Cu^{2+},[44] accompanied by an orange fluorescence turn-on response (Fig. 1). In sharp contrast, other metal cations examined in this work did not make any noticeable fluorescence spectral changes. This implied that the **1** can serve as a highly selective fluorescent probe for Cu^{2+} detection in a near pure water solution. To further exemplify its selectivity toward Cu^{2+}, the competition experiment was conducted. The result revealed that Cu^{2+} can induce the similar fluorescence enhancement of **1** in the presence of Hg^{2+}, Fe^{3+}, Co^{2+}, Cd^{2+}, Fe^{2+}, Ni^{2+}, Zn^{2+}, Pb^{2+}, Ca^{2+},

Mg^{2+}, K^{+}, and Na^{+}, without significant interference from these common metal cations (Fig. 2).

(Fig. 1. and **Fig. 2.)**

3.2. Effect of pH and response time

To get the optimal sensing condition of the probe **1** for Cu^{2+}, the pH effect and response time were firstly examined and the results were shown in Fig. 3 and Fig. 4. Without Cu^{2+}, the probe **1** only showed a weak fluorescence over all of pH range examined, but the enhanced fluorescence was observed in the presence of Cu^{2+} and remained almost constant in a wide pH range of 6–10 (Fig. 3). It is obvious that the wide pH range of 6–10 makes it possible to apply the probe **1** in the physiological pH window. Thus the Tris-HCl buffer solution (pH = 7.4, 10 mM) was chosen for the following experimental measurements. Fig. 4 showed that the time-dependent change of fluorescence intensity of **1** (10 μM) upon addition of 20 equiv Cu^{2+} in aqueous solution. It can be seen that the fluorescence intensity at 576 nm was continuously increased with standing time and leveled off until 60 min. Thus all measurements were carried out after standing the mixture solution for 60 min.

(Fig. 3. and **Fig. 4.)**

3.3. Fluorescence and absorption spectral titrations

Fig. 5 showed fluorescence and absorption titrations of **1** (10 μM) with Cu^{2+} in Tris-HCl buffer solution (pH = 7.4, 1% CH_3CN). As shown in Fig. 5a, the fluorescence intensity at 576 nm continuously increased with increasing concentrations of Cu^{2+} up to 20 equiv and saturated after that.

A similar trend was also observed in the absorption titration, where the visible absorption peak at 556 nm increased up to 20 equiv Cu^{2+} addition (Fig. 5b). A good linear relationship was found between the fluorescence intensity at 576 nm ($FI_{576\ nm}$) and the concentrations of Cu^{2+} over a range of 5–200 μM (R^2 = 0.9830, Fig. 6) with a detection limit of 2 μM (S / N = 3). This indicates that the **1** can serve as a highly sensitive fluorescent probe for Cu^{2+} detection in physiological conditions.

(Fig. 5. and **Fig. 6.)**

3.4. Preliminary application in living cells

To demonstrate its potential application in biological samples, the probe **1** was used for fluorescence imaging Cu^{2+} in living cells. Hela cells were firstly incubated with **1** (10 μM) for 30 min at 37 ^{o}C, then further incubated with the addition of Cu^{2+} (50 μM) for another 60 min and observed by using the fluorescence microscopy, respectively. As shown in Fig. 7, no significant fluorescence could be observed from the living cells incubated with the probe **1** only (Fig. 7a), but a bright orange fluorescence was observed when the cells were further incubated with Cu^{2+} (Fig. 7d). These results indicated that probe **1** can be applied for intracellular Cu^{2+} detection (Fig. S1).[45]

(Fig. 7.)

3.5. Investigation of sensing mechanism

To understand the sensing mechanism involved in this work, excess EDTA was added into the mixture aqueous solution of **1** and Cu^{2+}, and it was found that both the fluorescence and absorption

spectra did not show any noticeable change. This indicates that an irreversible reaction may occur between **1** and Cu^{2+} in aqueous solution. To investigate the coordination interaction between the probe **1** and Cu^{2+} ion, the fluorescence titration was performed in CH_3CN. It was found that the fluorescence of **1** increased with increasing Cu^{2+} concentration up to 1 equiv and saturated after that, implying a 1:1 stoichiometry that was further confirmed by Job's plot (Fig. S2). ESI-MS analysis of the mixture of **1** and 2 equiv of Cu^{2+} clearly showed a peak at *m/z* 575.1, corresponding to [**1** – 2H + Cu^{2+}]$^+$ species (Fig. S3a). These findings reveal that a 1:1 complex of **1**–Cu^{2+} was formed in CH_3CN. To clarify the binding mode of the probe **1** toward Cu^{2+}, the DFT calculation was performed for **1** and 1:1 complex of **1**–Cu^{2+}. As shown in Fig. 8, the probe **1** has a spirocyclic conformation, but the spirocycle was open in **1**–Cu^{2+} complex, where Cu^{2+} is coordinated to the proximal amide carbonyl and carboxylic oxygen atoms with a Cu–O distance of 1.98 and 1.91 Å respectively, and a near linear O–Cu–O conformation (∠O–Cu–O = 158.1º). Water was then added into the above **1**–Cu^{2+} complex solution and the mixture was again subjected to ESI-MS analysis. It was found that the **1**–Cu^{2+} complex peak (*m/z* 575.1) disappeared and one strong peak, corresponding to the rhodamine B (*m/z* 443.2), observed (Fig. S3b). Based on these experimental results, a possible sensing mechanism of coordination-promoted hydrolysis reaction was proposed and presented in Scheme 2.

(Fig. 8.)

(Scheme 2.)

4. Conclusions

In summary, we have designed and synthesized a new rhodamine-based chemodosimeter for

Cu^{2+} in aqueous solution. The probe displayed a Cu^{2+}-selective fluorescence enhancement in a near pure water solution (only containing 1% CH_3CN as co-solvent) with a wide pH range of 6–10. A linear relationship between fluorescence intensity and the concentrations of Cu^{2+} over a range of 5–200 μM with a detection limit of 2 μM. A sensing mechanism of coordination-promoted hydrolysis was proposed based on ESI-MS analysis and DFT calculation. The present chemodosimeter worked well in physiological conditions and was capable of applying for fluorescence imaging of Cu^{2+} in the living cells.

Acknowledgements

This work was financially supported by the Research Fund for the Doctoral Program of Higher Education of China (20120075120018), Innovation Program of Shanghai Municipal Education Commission (12ZZ067), and Fundamental Research Funds for the Central Universities. We thank Dr. Xue-Yan Cao and Prof. Xiang-Yang Shi for their kind assistances on the fluorescence imaging.

Supplementary data

Data of fluorescence titration in CH_3CN, ESI-MS analysis, ^1H NMR, ^{13}C NMR, and MS spectra of compounds **2** and **1** are available.

Notes and References

[1] R. Uauy, M. Olivares and M Gonzalez. *Am. J. Clin. Nutr.*, 1998, **67**, 952S–959S.

[2] D. Strausak, J. F. Mercer, H. H. Dieter, W. Stremmel and G. Multhaup. *Brain Res. Bull.*, 2001, **55**, 175–185.

[3] B. Valeur and I. Leray. *Coord. Chem. Rev.*, 2000, **205**, 3–40.

[4] D. T. Quang and J. S. Kim. *Chem. Rev.*, 2010, **110**, 6280–6301.

[5] A. P. De Silva, H. Q. N. Gunaratne, T. Gunnlaugsson, A. J. M. Huxley, C. P. McCoy, J. T. Rademacher and T. E. Rice. *Chem. Rev.*, 1997, **97**, 1515–1566.

[6] E. L. Que, D. W. Domaille and C. J. Chang. *Chem. Rev.*, 2008, **108**, 1517–1549.

[7] D. W. Domaille, E. L. Que and C. J. Chang. *Nat. Chem. Biol.*, 2008, **4**, 168–175.

[8] Y.-M. Yang, Q. Zhao, W. Feng and F.-Y. Li. *Chem. Rev.*, 2013, **113**, 192−270.

[9] X.-H. Li, X.-H. Gao, W. Shi and H.-M. Ma. *Chem. Rev.*, 2014, **114**, 590−659.

[10] L. D. Lavis and R. T. Raines. *ACS Chem. Biol.*, 2008, **3**, 142–155.

[11] J. R. Lakowicz. Principles of fluorescence spectroscopy. Springer, New York, 3rd edn, 2006.

[12] H. N. Kim, M. H. Lee, H. J. Kim, J. S. Kim and J. Yoon, *Chem. Soc. Rev.*, 2008, **37**, 1465–1472.

[13] X. Chen, T. Pradhan, F. Wang, J. S. Kim and J. Y. Yoon. *Chem. Rev.*, 2012, **112**, 1910–1956.

[14] H. Zheng, X.-Q. Zhan, Q.-N. Bian and X.-J. Zhang, *Chem. Commun.*, 2013, **49**, 429–447.

[15] Y. Zhao, X.-B. Zhang, Z.-X. Han, L. Qiao, C.-Y. Li, L.-X. Jian, G.-L. Shen and R.-Q. Yu. *Anal. Chem.*, 2009, **81**, 7022−7030.

[16] Y. Xiang, A.-J. Tong, P.-Y. Jin and Y. Ju. *Org. Lett.*, 2006, **8**, 2863–2866.

[17] X. Zhang, Y. Shiraishi and T. Hirai. *Org. Lett.*, 2007, **9**, 5039–5043.

[18] X. Zhang, S. Sumiya, Y. Shiraishi and T. Hirai. *J. Photochem. Photobiol. A*, 2009, **205**, 215–220.

[19] J. Zhang, C. Yu, S. Qian, G. Lu and J. Chen. *Dyes Pigm.*, 2012, **92**, 1370–1375.

[20] M.-Z. Tian, M.-M. Hu, J.-L. Fan, X.-J. Peng, J.-Y. Wang and S.-G. Sun. *Bioorg. Med. Chem. Lett.*, 2013, **23**, 2916–2919.

[21] X.-Y. Guan, W.-Y. Lin and W.-M. Huang. *Org. Biomol. Chem.*, 2014, **12**, 3944–3949.

[22] P. Puangploy, S. Smanmoo and W. Surareungchai. *Sens. Actuators B*, 2014, **193**, 679–686.

[23] M. Wang, F.-Y. Yan, Y. Zou, L. Chen, N. Yang and X.-G. Zhou. *Sens. Actuators B*, 2014, **192**, 512–521.

[24] Y.-K. Yang, K.-J. Yook and J. Tae, *J. Am. Chem. Soc.*, 2005, **127**, 16760–16761.

[25] X. Zhang, Y. Shiraishi and T. Hirai. *Tetrahedron Lett.*, 2007, **48**, 5455–5459.

[26] X. Zhang, Y. Shiraishi and T. Hirai. *Tetrahedron Lett.*, 2008, **49**, 4178–4181.

[27] X. Zhang, X.-J. Huang and Z.-J. Zhu. *RSC Adv.*, 2013, **3**, 24891–24895.

[28] X. Zhang and Y.-Y. Zhu. *Sens. Actuators B*, 2014, **202**, 609–614.

[29] H. Wen, Q. Huang, X.-F. Yang and H. Li. *Chem. Commun.*, 2013, **49**, 4956–4958.

[30] L. Wang, J. Yan, W. Qin, W. Liu and R. Wang. *Dyes Pigm.*, 2012, **92**, 1083–1090.

[31] V. Dujols, F. Ford and A.W. Czarnik, *J. Am. Chem. Soc.*, 1997, **119**, 7386–7387.

[32] M.-X. Yu, M. Shi, Z.-G. Chen, F.-Y. Li, X.-X. Li, Y.-H. Gao, J. Xu, H. Yang, Z.-G. Zhou, T. Yi and C.-H. Huang. *Chem. Eur. J.*, 2008, **14**, 6892–6900.

[33] Z.-Q. Hu, X.-M. Wang, Y.-C. Feng, L. Ding and H.-Y. Lu. *Dyes Pigm.*, 2011, **88**, 257–261.

[34] S. K. Kempahanumakkagaari, R. Thippeswamy and P. Malingappa. *J. Lumin.*, 2014, **146**, 11–17.

[35] M. Kumar, N. Kumar, V. Bhalla, P. R. Sharma and T. Kaur. *Org. Lett.*, 2012, **14**, 406–409.

[36] L. Yuan, W.-Y. Lin, B. Chen and Y.-N. Xie. *Org. Lett.*, 2012, **14**, 432–435.

[37] Z.-H Jiang, S.-J. Tian, C.-Q Wei, T. Ni, Y. Li, L. Dai and D.-Z. Zhang. *Sens. Actuators B*, 2013, **184**, 106–112.

[38] F.-J. Huo, L. Wang, C.-X. Yin, Y.-T. Yang, H.-B. Tong, J.-B. Chao and Y.-B. Zhang. *Sens. Actuators B*, 2013, **188**, 735–740.

[39] M. Li, H.-S. Lv, J.-Z. Luo, J.-Y. Miao and B.-X. Zhao. *Sens. Actuators B*, 2013, **188**, 1235–

1240.

[40] J.-X. Yin, X. Ma, G.-H. Wei, D.-B Wei and Y.-G. Du. *Sens. Actuators B*, 2013, **177**, 213–217.

[41] K. Kaur, R. Saini, A. Kumar, V. Luxami, N. Kaur, P. Singh and S. Kumar. *Coord. Chem. Rev.*, 2012, **256**, 1992–2028.

[42] J.-J. Du, M.-M. Hu, J.-L. Fan and X.-J. Peng. *Chem. Soc. Rev.*, 2012, **41**, 4511–4535.

[43] M. J. Frisch, G. W. Trucks, H. B. Schlegel, G. E. Scuseria, M. A. Robb, J. R. Cheeseman, G. Scalmani, V. Barone, B. Mennucci, G. A. Petersson, H. Nakatsuji, M. Caricato, X. Li, H. P. Hratchian, A. F. Izmaylov, J. Bloino, G. Zheng, J. L. Sonnenberg, M. Hada, M. Ehara, K. Toyota, R. Fukuda, J. Hasegawa, M. Ishida, T. Nakajima, Y. Honda, O. Kitao, H. Nakai, T. Vreven, J. A. Montgomery, Jr., J. E. Peralta, F. Ogliaro, M. Bearpark, J. J. Heyd, E. Brothers, K. N. Kudin, V. N. Staroverov, T. Keith, R. Kobayashi, J. Normand, K. Raghavachari, A. Rendell, J. C. Burant, S. S. Iyengar, J. Tomasi, M. Cossi, N. Rega, J. M. Millam, M. Klene, J. E. Knox, J. B. Cross, V. Bakken, C. Adamo, J. Jaramillo, R. Gomperts, R. E. Stratmann, O. Yazyev, A. J. Austin, R. Cammi, C. Pomelli, J. W. Ochterski, R. L. Martin, K. Morokuma, V. G. Zakrzewski, G. A. Voth, P. Salvador, J. J. Dannenberg, S. Dapprich, A. D. Daniels, O. Farkas, J. B. Foresman, J. V. Ortiz, J. Cioslowski and D. J. Fox, *Gaussian 09, Revision C.01*, Gaussian, Inc., Wallingford CT, 2010.

[44] The fluorescence quantum yield of the probe **1** was determined to be 0.05 and 0.49 in the absence and presence of 20 equiv Cu^{2+} respectively by using rhodamine B as standard (Φ_F = 0.69 in ethanol, C. A. Parker and W. T. Rees. *Analyst*, 1960, **85**, 587–600).

[45] The Recommended Dietary Allowance (RDA) of copper for adults is 900 μg per day, but the normal level is 10–25 μM for serum copper concentration and 180 to 400 mg L^{-1} for ceruloplasmin concentration (National Research Council. Dietary Reference Intakes for Vitamin

A, Vitamin K, Arsenic, Boron, Chromium, Copper, Iodine, Iron, Manganese, Molybdenum, Nickel, Silicon, Vanadium, and Zinc. The National Academies Press, Washington DC, 2001, 224–227). Additionally, the US Environmental Protection Agency (EPA) has set the maximum allowable level of copper in drinking water at 1.3 ppm (ca. 20 μM). To further demonstrate the sensitivity of the probe **1**, it was then used for fluorescence imaging 20 μM Cu^{2+} in living cells and the orange fluorescence signal was still discernible (Fig. S1).

Figure Captions:

Scheme 1. Synthesis procedure of the probe **1**.

Scheme 2. Proposed sensing mechanism involved in this work.

Fig. 1. Fluorescence response of **1** (10 μM) toward 20 equiv various metal cations in Tris-HCl buffer solution (pH = 7.4, 1% CH_3CN). Insets are the corresponding fluorescence spectral and color changes. Excitation and emission wavelengths are 520 and 576 nm, respectively.

Fig. 2. Change in the fluorescence intensity of **1** (10 μM) upon addition of 20 equiv Cu^{2+} in the absence (black column) and presence (red column) of 20 equiv various metal cations in Tris-HCl buffer solution (pH = 7.4, 1% CH_3CN). Excitation and emission wavelengths are 520 and 576 nm, respectively.

Fig. 3. Effect of pH on the fluorescence intensity of **1** (10 μM) in the absence and presence of 20 equiv Cu^{2+} in the aqueous solution (1% CH_3CN). Excitation and emission wavelengths are 520 nm and 576 nm, respectively.

Fig. 4. Time dependent change of the fluorescence intensity of **1** (10 μM) upon addition of 20 equiv of Cu^{2+} in Tris-HCl buffer solution (pH = 7.4, 1% CH_3CN). Excitation and emission wavelengths are 520 and 576 nm, respectively.

Fig. 5. Fluorescence (a) and absorption (b) titrations of **1** (10 μM) with Cu^{2+} in Tris-HCl buffer solution (pH = 7.4, 1% CH_3CN). Excitation wavelength in (a) is 520 nm.

Fig. 6. Plots of fluorescence intensity of **1** (10 μM) versus amounts of Cu^{2+} in Tris-HCl buffer solution (pH = 7.4, 1% CH_3CN). Excitation and emission wavelengths are 520 and 576 nm, respectively.

Fig. 7. Confocal fluorescence (a, d), bright field (b, e), and overlay images (c, f) of Hela cells, incubated with **1** (10 μM) for 30 min at 37 ^oC (a–c) and further incubated with addition of Cu^{2+} (50 μM) for another 60 min at 37 ^oC (d–f), respectively.

Fig. 8. The optimized structures of **1** and 1:1 complex of **1**–Cu^{2+} from DFT calculation. Gray, red, blue and pink atoms denote C, O, N and Cu atoms, respectively, where H atoms are omitted for clarity.

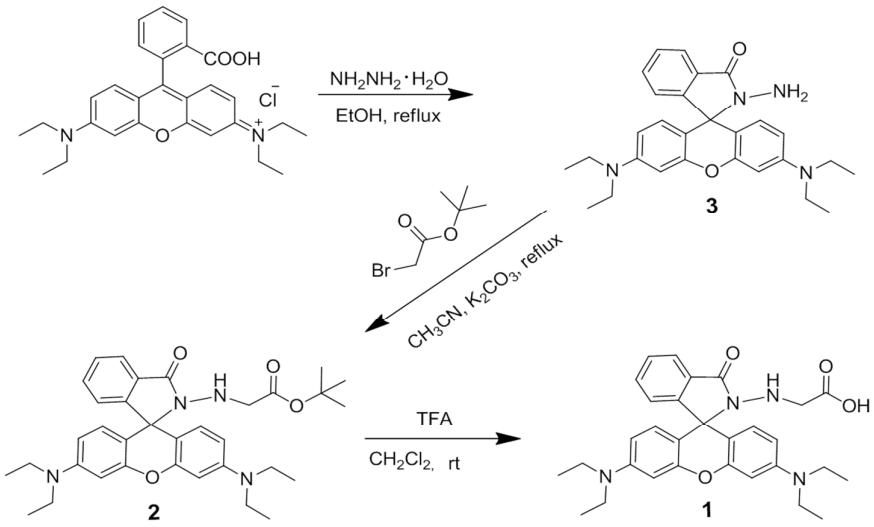

Scheme 1

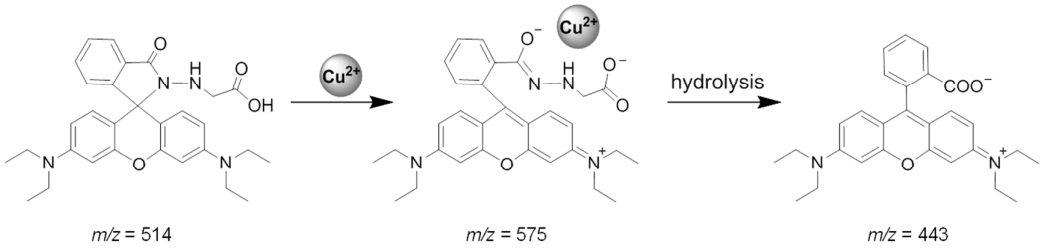

Scheme 2

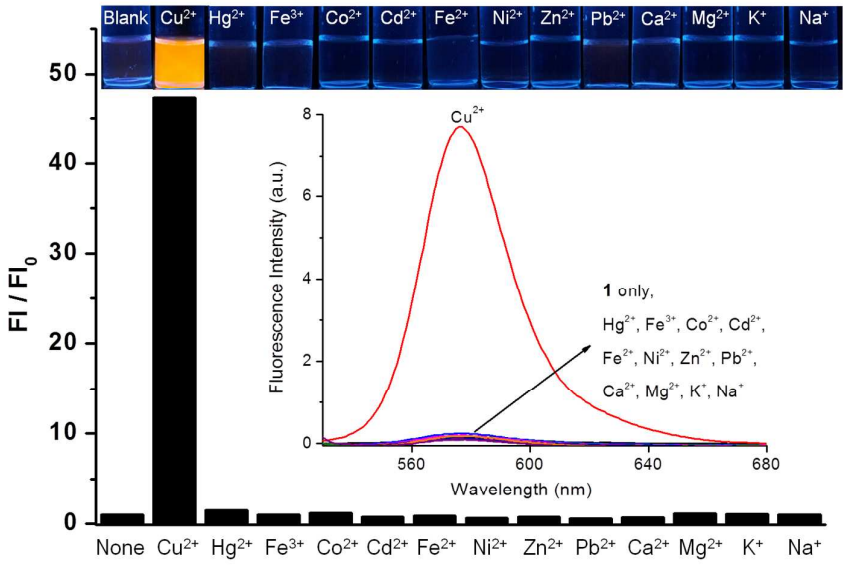

Fig. 1

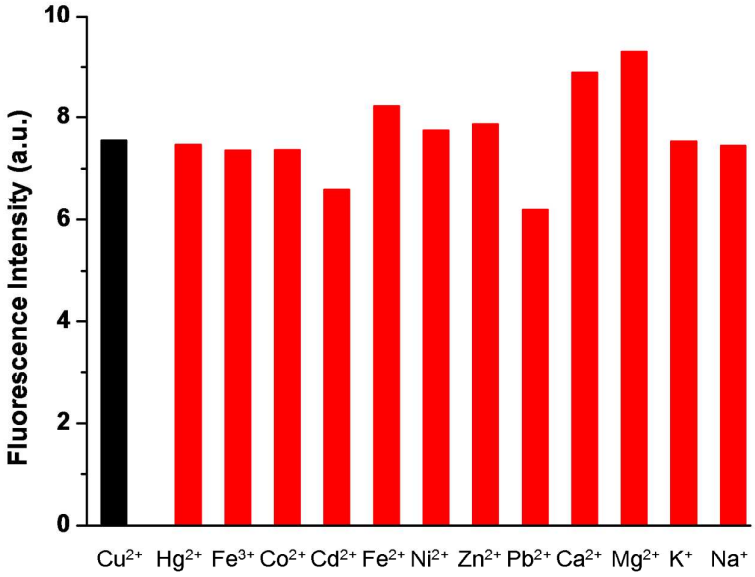

Fig. 2

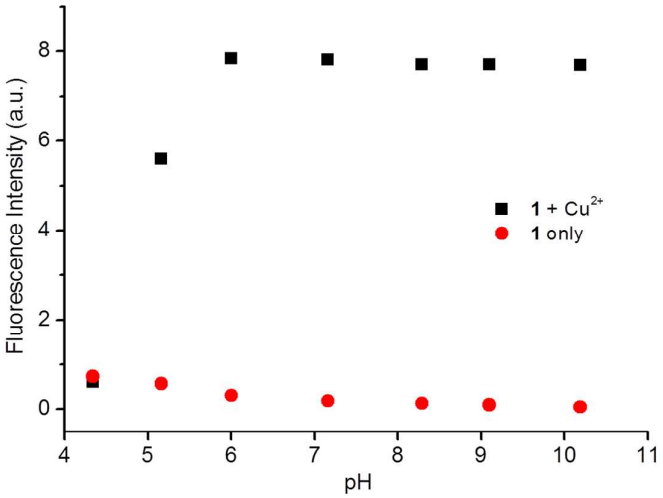

Fig. 3

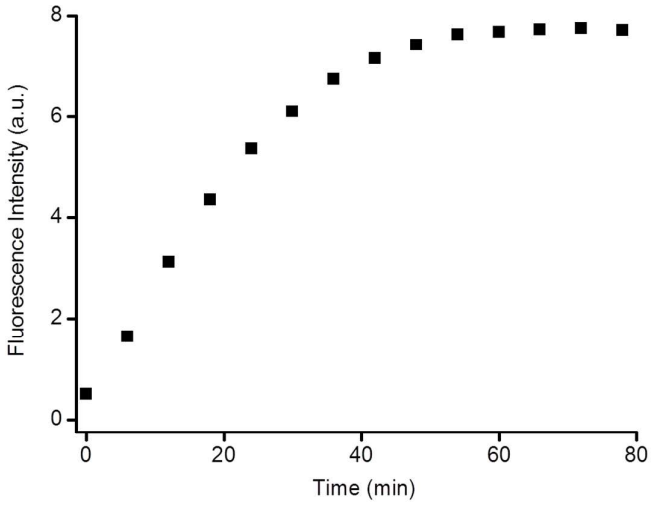

Fig. 4

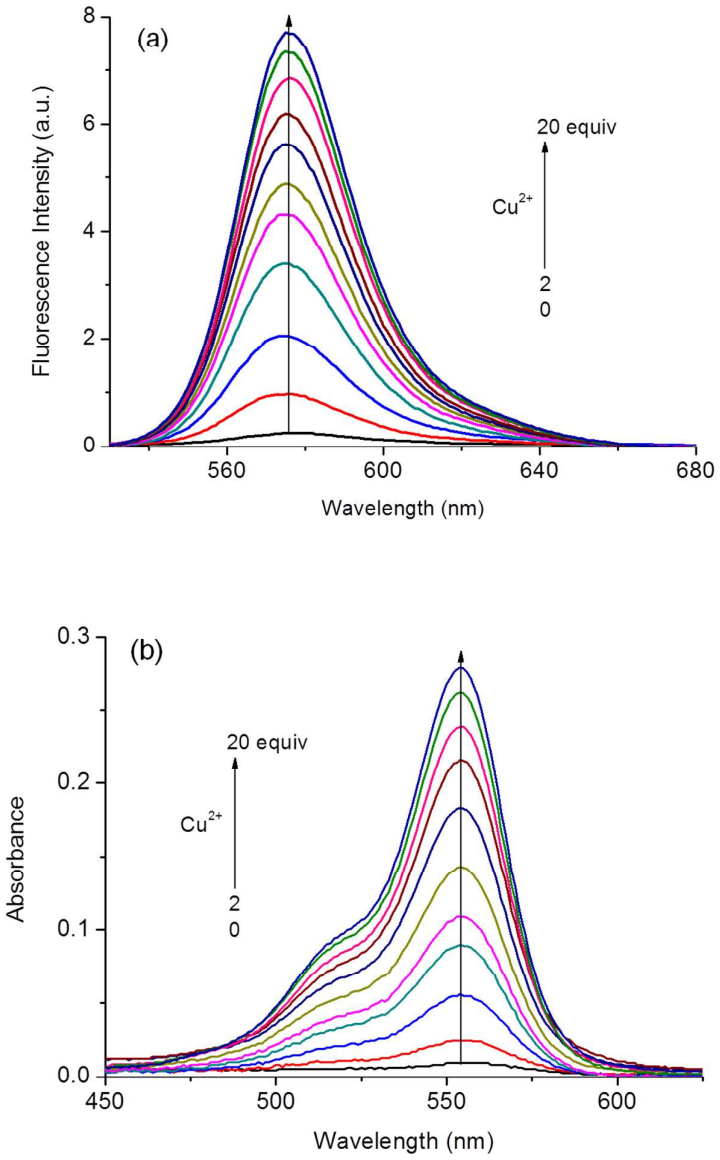

Fig. 5

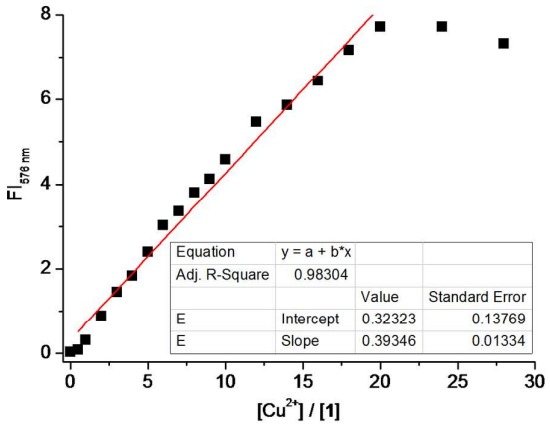

Fig. 6

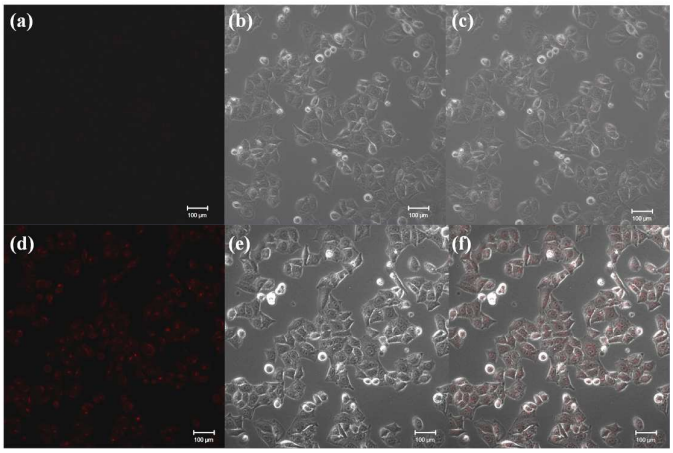

Fig. 7

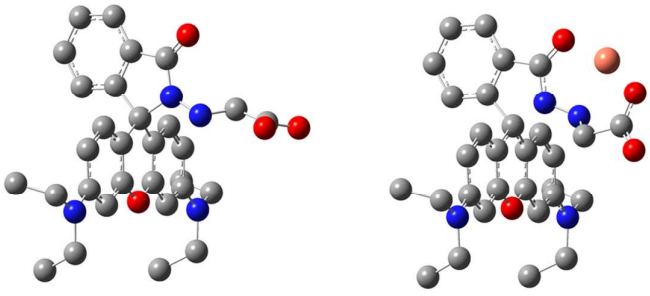

Fig. 8